Tetrahedron 69 (2013) 7683–7691

Contents lists available at SciVerse ScienceDirect

Tetrahedron

journal homepage: www.elsevier.com/locate/tet

Template-induced macrocycle diversity through large ring-forming alkylations of tryptophan

Kenneth V. Lawson, Tristan E. Rose, Patrick G. Harran *

Department of Chemistry and Biochemistry, University of California Los Angeles, 607 Charles E. Young Drive East, Los Angeles, CA 90095-1569, USA

ARTICLE INFO

Article history:
Received 8 March 2013
Received in revised form 14 May 2013
Accepted 16 May 2013
Available online 23 May 2013

Keywords:
Peptidomimetic
Macrocycle
Friedel–Crafts
Diversity
NMR solution structure

ABSTRACT

Macrocyclic peptidomimetics are valuable in research and serve as lead compounds in drug discovery efforts. New methods to prepare such structures are of considerable interest. In this pilot study, we show that an organic template harboring a latent cinnamyl cation participates in novel Friedel–Crafts macrocyclization reactions with tryptophan. Upon joining the template to Trp-Trp-Tyr, a single operation efficiently generates eight unique macrocycles. Each has been isolated and thoroughly characterized. Product distribution as a function of Brønsted and/or Lewis acidic conditions was explored, and outcomes were compared to rearrangements induced within a corresponding tyrosine-linked cyclic ether. The solution structure of a new macrocyclic pyrroloindoline was solved using a combination of two-dimensional NMR methods and molecular mechanics simulations. Template-induced structural diversification of peptide sequences harboring aromatic residues has potential to create myriad macrocycles that target surfaces involved in protein–protein interactions.

1. Introduction

As opportunities in biological research and drug discovery expand, there is a considerable need for synthetic methods that form new types of complex small molecules.[1] Conventional screening libraries often fail to produce viable lead structures when challenged with demanding targets.[2] These include receptors with relatively large, dynamic, or solvent exposed ligand binding sites and protein–protein interaction surfaces.[3] Recent drug discovery efforts aimed at such targets[4] have benefited from biophysical studies highlighting 'hot spots' within these larger binding motifs.[5] Focused libraries that incorporate structures able to interact selectively and avidly with such sites would be valuable. Molecules that recapitulate the three-dimensional display of functional groups found in native binding partners while possessing favorable pharmacological properties would be ideal.

Peptides are intrinsically relevant to this goal. They are a logical starting point to identify ligands for protein surfaces.[6] However, peptides frequently exhibit poor bioavailability and limited stability in vivo.[7] Numerous strategies have been developed to mitigate these problems, including the incorporation of D-configured[8] and non-proteinogenic amino acids,[9] pseudo-peptide bonds, and conformational constraints.[10,11] Each of these features is seen in peptide-derived macrocyclic natural products, which often possess markedly different properties relative to their acyclic precursors. With macrocycles as a central theme, we have sought to expand upon existing methods for large ring formation.

In a previous report, we outlined elements of a program aimed at systematically generating complex peptidomimetics.[12] These experiments used designed templates (Fig. 1B) to form composite structures with peptides.[13] Our current templates capitalize on reactivity of the cinnamyl cation, and transiently formed palladium

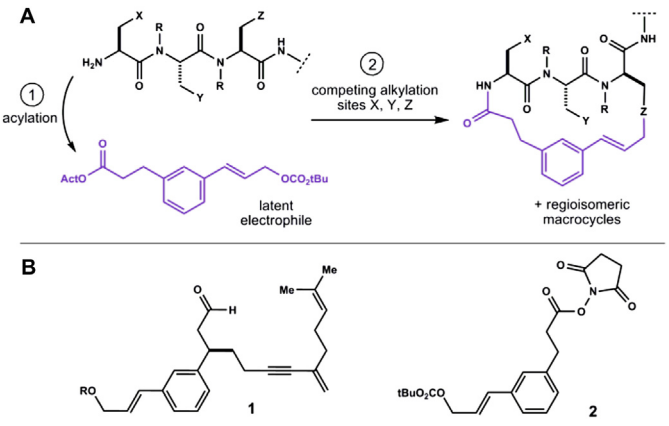

Fig. 1. (A) Current template designs (purple) utilize a cinnamyl mixed carbonate as a latent electrophile. Competing reactions with side-chain nucleophiles provide isomeric macrocycles of varying shape, (B) prototypical templates **1** and **2** (this work). R=$CO_2CMe_2CCl_3$.

* Corresponding author. Tel.: +1 310 825 6578; fax: +1 310 206 0204; e-mail address: harran@chem.ucla.edu (P.G. Harran).

0040-4020/$ – see front matter © 2013 Elsevier Ltd. All rights reserved.
http://dx.doi.org/10.1016/j.tet.2013.05.060

complexes thereof, to efficiently promote large ring-forming substitution reactions involving aromatic rings and heteroatom nucleophiles. While numerous methods exist to prepare peptidic macrocycles, most require tailored reacting partners.[10a,14,15] Our template chemistry exploits reactivity inherent to a subset of natural amino acid side chains.

For example, we used the allylic carbonate in template **1** (Fig. 1B) to form macrocyclic ethers by engaging the phenol of tyrosine in palladium catalyzed substitution reactions.[12,16] In the context of peptides harboring other aromatic residues, we observed that acid treatment caused these ethers to rearrange, wherein the cinnamyl unit migrated to adjacent tryptophan residues forming stable carbon–carbon bonded products. This was an exciting discovery. To probe this reactivity in greater detail, and in systems not complicated by competing rearrangements of the diene-yne appendage in **1**, we synthesized template **2**.[17] Using simple, straightforward chemistry, composites of **2** participate in remarkable reactions that alter the structure and properties of linear peptide motifs (vide infra).

Toward the goal of rapidly accessing diverse, natural product-like structures, we demonstrate use of **2** in a divergent process to prepare mixtures of macrocyclic products displaying a peptidic binding epitope.[18] In two synthetic steps, template **2** transforms a peptide harboring multiple nucleophilic side-chains (X, Y, Z Fig. 1A) into constitutionally isomeric macrocycles through competing reaction pathways. The resulting products differ in core ring size and conformation, each dictating a unique display of side chains.[19] The structural diversity derived from this process arises from the nature of the starting peptide and the reactivity of the template. Processes of this kind have potential to create composite macrocycles with inherent complementarity to protein surfaces.

2. Results and discussion

2.1. Preparation of cyclic and acyclic acidolysis precursors

Template **2** was prepared from commercial 3-(3-bromophenyl) propionic acid in six steps and 51% overall yield.[17] This material acylated the N-terminus of synthetic Trp-Trp-Tyr-NH_2 without incident, providing composite product **4** in good yield (Fig. 2). Analogous to previous work, exposure of **4** to 5 mol % $Pd(PPh_3)_4$ catalyzed efficient macrocyclization to give tyrosine O-linked cinnamyl ether **5**. Treatment of **5** with 15 equiv methanesulfonic acid in anhydrous nitromethane at room temperature provided a mixture of three isolable products (Figs. 3A and 5B). These proved to be analogous to the four macrocyclic core structures observed previously from reactions of template **1** with Trp-Trp-Tyr-NH_2.[12]

Close inspection of HPLC–MS ion chromatograms indicated the presence of five additional minor isomers (vide infra). Combined, those eight products accounted for >95% of the total peak area (HPLC–UV at 254 nm). This confirmed that template **2** was an excellent model for further study.

2.2. Purification and characterization

Acidolysis products **6**–**12** were readily separated by reverse phase preparative HPLC (Fig. 5). From macrocyclic ether **5**, we initially isolated only **6**, **7**, and **11** in sufficient quantities for NMR analyses. Upon refining the reaction conditions (see Section 2.3 and Table 1), initially trace components **8**, **9**, **10**, and **12** were also isolated. Compounds **6**–**9**, **11**, and **12** were each obtained in >95% purity. Only fraction **10** was isolated as a mixture of closely related regioisomers **10a** and **10b**, which were characterized together.

The planar structures of compounds **6**–**12** (Fig. 3A) were determined by complete assignment of their proton and carbon connectivities on the basis of homo- and heteronuclear correlations obtained from 2D and selective 1D NMR experiments (see Supplementary data). Structural elucidation involved (1) sequential assignment of the peptide backbone, (2) correlation of backbone atoms to their corresponding side chain aromatic ring, and (3) determination of the connectivity of the cinnamyl moiety to an aromatic side chain.

In this model peptide, complete resonance assignment of the peptide was required to differentiate between the two tryptophan residues. Sequential assignment of the amide backbone was made by H^N–C(O) and H^α–C(O) correlations observed by HMBC,[20] or by H^α_i–H^N_{i+1} NOE where ambiguities arose from weak correlations or overlapping carbonyl resonances.[21] Assignment of residue specific H^N–H^α–H^β spin systems from TOCSY spectra was then possible,[22] and connectivity of H^β to the aromatic portion of the side chain was established from reciprocal HMBC correlations.

The ansa bridge motif arising from electrophilic aromatic substitution causes a characteristic loss of one proton relative to the parent ^1H spin system of the aromatic amino acid side chains, which was apparent by TOCSY. The precise position of substitution was deduced from careful analysis of $^{2,3,4}J_{CH}$ correlations observed in HMBC experiments (e.g., Fig. 4A). In general, heteronuclear correlations from the cinnamyl methylene to aromatic resonances of the substituted ring, and the reciprocal thereof, allowed unambiguous structural assignment. In cases where HMBC correlations were either unclear or not observed, the connectivity of the cinnamyl unit was inferred from NOE correlations between the two proximal spin systems observed by TOCSY (Fig. 4B).

The isomeric products obtained from acidolysis of macrocyclic ether **5** comprised three of the four outcomes anticipated from previous work. We obtained compound **6**, arising from rearrangement of the O-linked macrocyclic ether to the phenolic *ortho* position, as the predominant product. The next most abundant

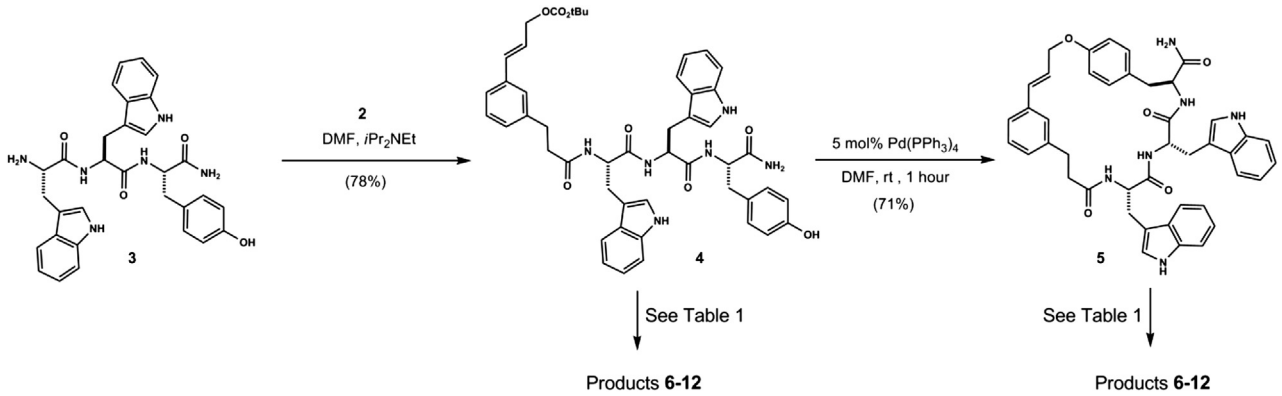

Fig. 2. Reaction conditions: (a) H-Trp-Trp-Tyr·TFA (1 equiv), template **2** (1 equiv), $^iPr_2NEt$ (4 equiv), DMF (0.1 M). (b) $Pd(PPh_3)_4$ (5 mol %), DMF (5 mM, degassed).

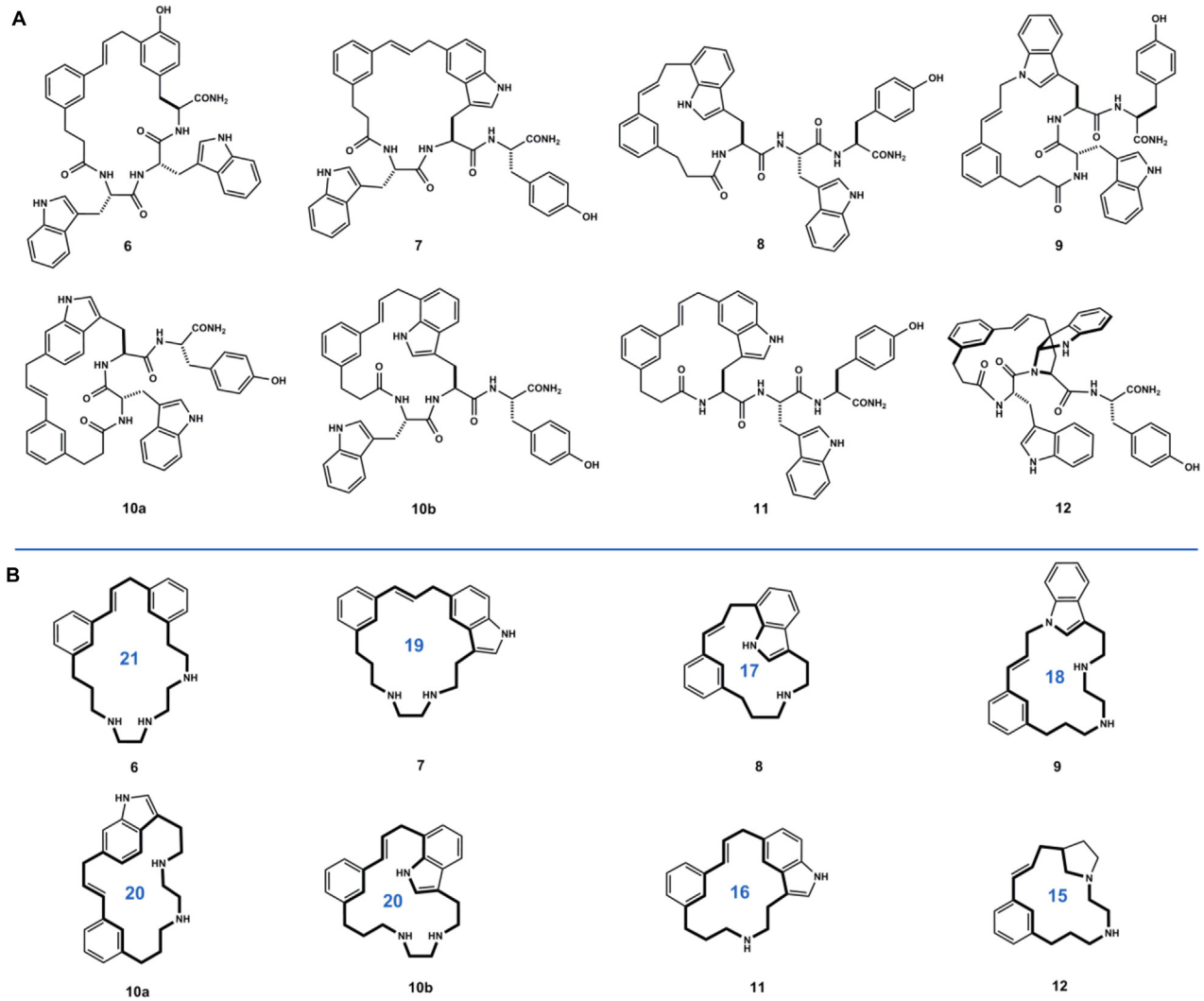

Fig. 3. (A) Products obtained and fully characterized from acidolysis of **4** and **5**. For conditions and relative yields see Table 1. (B) Macrocyclic core structures **6**–**12** have, to our knowledge, not been reported in the literature.

outcomes derived from alkylation of tryptophan at indole C5. Substitution of Trp1 (**11**) and Trp2 (**7**) at indole C5 comprised 17% and 7% of the product mixture, respectively. The absence of branched isomers observed previously from alkylation at indole C2 likely reflects a subtle difference between the conformational preferences of templates **1** and **2**.[12]

2.3. Unprecedented large ring-forming Friedel–Crafts alkylations

We next investigated what role the cinnamyl ether in **5** played in the formation of carbon–carbon bonded isomers. Acid promoted rearrangement of cyclic ether **5** to isomers **6**–**12** is, for this substrate, a set of competing ring contractions. It was possible that starting from a pre-organized cyclic template like **5** was necessary to observe such outcomes. Large ring-forming Friedel–Crafts alkylations are virtually absent from the literature.[23,24] To test this idea, we subjected acyclic mixed carbonate **4** to the same reaction conditions that caused isomerizations of **5**. Remarkably, the reaction afforded a mixture of products that co-chromatographed with those derived from **5**, varying only in their relative abundance (Fig. 5A). From this more evenly-distributed mixture, minor products **8**, **9**, **10a**/**b**, and **12** were readily isolated and characterized. Structure elucidation by NMR methods led to the assignment of five novel macrocycles arising from alkylation of tryptophan at indole N1, C3, C6, and C7. Products of C5 alkylation of Trp1 (**11**) and Trp2 (**7**) were obtained as the major products, consistent with the relatively high reactivity of this position observed in rearrangement of **5**, and in related bimolecular reactions.[25] Tyrosine alkylation product **6**, the major product from **5**, now comprised only 12% of the product mixture. Lesser products arising from alkylation at C7 of Trp1 (**8**) and Trp2 (**10b**), C6 of Trp2 (**10a**), and N1 of Trp2 (**9**) were also obtained. Product **12**, comprising the final 12% of the mixture, was determined to be a macrocyclic pyrroloindoline arising from indole C3 alkylation of Trp2 and trapping of the resultant indolium ion by the proximal amide nitrogen (Fig. 6).[26]

Template **2** illustrates the utility of the cinnamyl cation to access diverse macrocycles by direct engagement of aromatic amino acid side chains. From a single reaction, we isolated eight unique macrocyclic cores comprising 15, 16, 17, 18, 19, 20, and 21-membered rings (see Fig. 3B). Isomeric structures **6**–**12** exhibit varying polarity as evidenced by their elution order in HPLC, and distinct conformations as evidenced by large chemical shift differences observed between conserved motifs (see Supplementary data). These results bode well for accessing molecular diversity by template-induced macrocyclization of oligomers containing other π-basic aromatic residues.

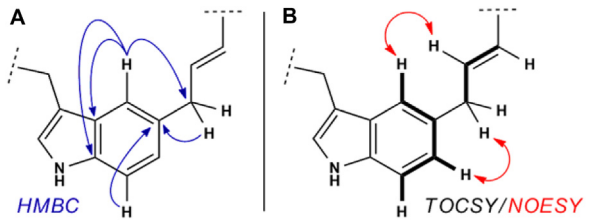

Fig. 4. Connectivity of macrocycles was determined from (A) HMBC or (B) TOCSY and NOESY/ROESY correlations, as illustrated for tryptophan indole C5 alkylation products **7** and **11**.

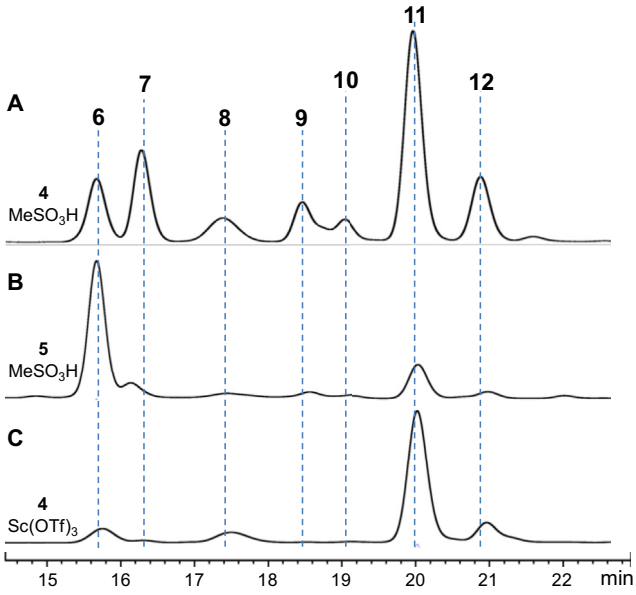

Fig. 5. HPLC traces of large-ring forming reactions: (A) **4** with $MeSO_3H$ (conditions: Table 1, entry 11), (B) **5** with $MeSO_3H$ (conditions: Table 1, entry 3), (C) **4** with $Sc(OTf)_3$ (conditions: Table 1, entry 17). Conditions: RP-C18, $MeCN/H_2O$, 0.1% TFA (see Supplementary data).

2.4. Affects of acid catalyst, solvent, and pre-cyclization

Counterion and solvent effects are known to perturb the reaction rate and product distributions of Friedel–Crafts alkylation and rearrangement reactions.[27] Accordingly, we examined alternative conditions to promote large ring-forming reactions of mixed carbonate **4** and cyclic cinnamyl ether **5**.

The nature of the acidic counterion was examined using a range of Brønsted and Lewis acids in both polar and non-polar solvents, the results of which are summarized in Table 1. Strong organic acids, including methanesulfonic acid and trifluoroacetic acid (TFA) were superior in promoting clean conversion to products **6**–**12** by ring contractions of **5** (entries 1–10) and direct large-ring formations from **4** (entries 11–17). Weaker acids, such as aqueous acetic acid (not shown) and formic acid, returned only the starting material. Using methanesulfonic acid, but changing the solvent from $MeNO_2$ to CH_2Cl_2, led to intractable decomposition of **4** as observed by HPLC–MS. Consistent with previous studies by Olah and others, nitromethane likely stabilizes ion-paired intermediates along the reaction pathway.[28] In CH_2Cl_2, stoichiometric amounts of TFA reacted only slowly, whereas higher concentrations of TFA rapidly converted both **4** and **5** to well-distributed mixtures comparable to those seen in reactions of **4** with methanesulfonic acid in nitromethane. Superacids showed mixed results. Stoichiometric triflic acid caused decomposition of **4** to non-isomeric products, even in $MeNO_2$ solvent. On the other hand, 2 equiv of bistriflimide caused rapid reaction of **4**, and doubled the relative abundance of pyrroloindoline **12**. Lewis acids also efficiently promoted these reactions. Relative to Brønsted acids, metal triflates, such as $Sc(OTf)_3$ enhanced the conversion of acyclic precursor **4** to Trp1 indole C5 alkylation product **11** (see Fig. 5C and Fig. S2). The product distribution from reactions of **4** is tunable with choice of acid promoter and solvent.

Under certain reaction conditions, significantly different product distributions were observed when starting from cyclic ether **5** relative to **4**. Reaction of **5** with dilute TFA in CH_2Cl_2 at room temperature (entry 9, Table 1), while sluggish, selectively formed tyrosine alkylation product **6**, exhibiting a prominent reversal of selectivity relative to that of **4** (entry 13).[29] This selectivity was lost at high concentrations of TFA. Similar trends were observed with methanesulfonic acid. Using only 5 equiv of methanesulfonic acid in nitromethane at −20 °C, **6** was formed in a 20:1 ratio relative to all other isomers. These dramatic differences appear to reflect the influence of conformational pre-organization in **5** on the resulting reaction pathways.

One way to rationalize these results is in terms of a qualitative least motion argument.[30] All else considered equal, the

Table 1
Effect of substrate and acid promoter on product distribution in rearrangement reactions of cyclic ether **5** and direct large-ring closure reactions of acyclic mixed carbonate **4**. Reaction conditions: substrate (5 mM) in indicated solvent, 2 h unless otherwise noted. Bold signifies substantial changes in product distribution has occurred

Entry	Substrate	Promoter	Equiv	Temp	Solvent	Compound%						
						6	**7**	**8**	**9**	**10**	**11**	**12**
1	5	$MeSO_3H$	5	rt	$MeNO_2$	74	4	3	3	1	12	3
2	5	$MeSO_3H$	15	0 °C	$MeNO_2$	71	6	3	2	2	13	3
3	5	$MeSO_3H$	15	rt	$MeNO_2$	63	7	4	3	2	17	4
4	5	$MeSO_3H$	25	−20 °C	$MeNO_2$	58	10	4	3	2	20	4
5[a]	5	$MeSO_3H$	5	−20 °C	$MeNO_2$	**95**	<1	<1	<1	<1	4	<1
6	5	$MeSO_3H$	15	rt	CH_2Cl_2	N/A[b]	—	—	—	—	—	—
7[a]	5	CF_3SO_3H	15	rt	CH_2Cl_2	N/A[b]	—	—	—	—	—	—
8	5	TFA	50% *v*	rt	CH_2Cl_2	3	24	8	15	3	34	13
9	5	TFA	15	rt	CH_2Cl_2	**95**	<1	<1	<1	<1	4	<1
10	5	$Sc(OTf)_3$	1	rt	$MeNO_2$	61	3	6	2	1	22	5
11	4	$MeSO_3H$	15	rt	$MeNO_2$	12	16	6	9	5	40	12
12	4	TFA	50% *v*	rt	CH_2Cl_2	32	17	7	7	1	28	8
13[a]	4	TFA	15	rt	CH_2Cl_2	21	14	6	7	5	35	11
14	4	CF_3SO_3H	1	rt	$MeNO_2$	N/A[b]	—	—	—	—	—	—
15	4	HCO_2H	50% *v*	rt	H_2O	NR	—	—	—	—	—	—
16[c]	4	Tf_2NH	2	rt	$MeNO_2$	4	14	5	8	6	38	**24**
17	4	$Sc(OTf)_3$	1	rt	$MeNO_2$	9	1	9	<1	<1	**68**	13

[a] 16 h reaction time.
[b] Decomposition to non-isomeric products observed.
[c] 30 min reaction time.

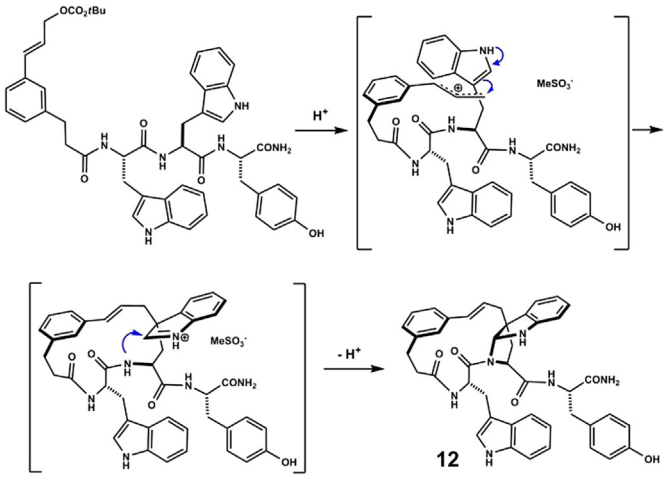

Fig. 6. Plausible mechanism for the formation of **12** involving initial alkylation of C3 of tryptophan followed by internal capture of the incipient iminium ion.

conformationally pre-organized template in **5** rearranges more selectively, with the cinnamyl unit migrating to electron rich positions adjacent to the original attachment site.[31] In contrast, ionization of acyclic carbonate **4** occurs in the context of a complex ensemble of peptide conformations, providing ample opportunity for the solvated cinnamyl ion pair to approach multiple internal reactive sites, wherein less selectivity is manifest and a more diverse mixture results.[32] The attenuated selectivity observed from **5** in higher concentrations of acid may reflect accelerated ion pair return or altered solvation thereby permitting relaxation away from the cyclic conformation and leading to products by similar pathways as **4**.[33]

While the initial acidolysis conditions using methanesulfonic acid gave a desirable, evenly-distributed product mixture, there are reasons to perturb this outcome. To retain tractability in biological screening exercises, a mixture should optimally contain an equal concentration of products so as to minimize the incidence of false negatives. Conversely, in the event that a single component becomes desirable as a result of either structure or function, it may be possible to enhance its abundance by subtle changes in reaction conditions, rather than undertaking a target-oriented synthesis. We have shown this is possible by biasing the template-induced macrocyclization toward the 15-membered macrocyclic pyrroloindoline **12**, 16-membered ring **11**, or 21-membered ring **6**. Cyclic cinnamyl ether **5** was essential in this regard. While we were successful in biasing the product distribution in favor of initially abundant compounds **6**, **11** or **12**, it is not yet clear this can be accomplished for minor constituents to the same degree. Further experiments on a variety of substrates are ongoing.

2.5. Deuterium labeling—mass spectrometry assay

The process of isolation and characterization of individual products derived from divergent acidolysis becomes challenging with increasingly sophisticated templates. Accordingly, we sought to develop sensitive analytical means to assess product distribution and the efficiency of large ring formations. In principle, perdeuteration of selected aromatic amino acid side-chains would provide a characteristic molecular mass shift upon electrophilic aromatic substitution by loss of $^2H^+$ upon re-aromatization (Fig. 7A). The high sensitivity of HPLC–MS would allow analytical separation of small-scale reactions. Successful aromatic substitution of the ^2H labeled amino acid would result in a molecular mass of [M−1].[34] To

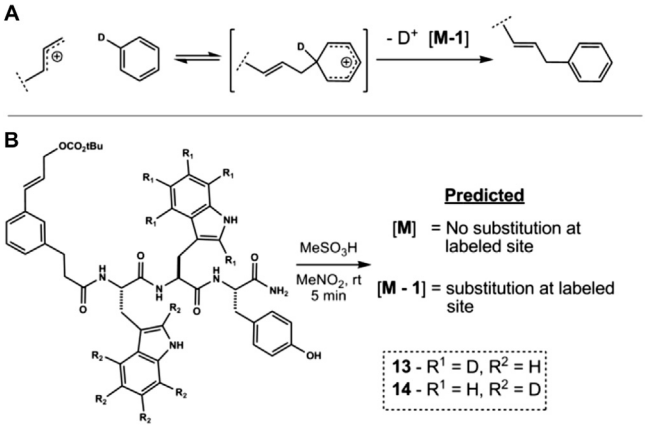

Observed

	6-d_5	7-d_5	8-d_5	9-d_5	10-d_5	11-d_5	12-d_5
13	[M]	[M-1]	[M]	[M-2]	[M-1]	[M]	[M]
14	[M]	[M]	[M-1]	[M]	[M]	[M-1]	[M]

Fig. 7. Selectively deuterated substrates permit sensitive detection of electrophilic substitution events by crude HPLC/MS analyses.

examine the viability of this approach, the tripeptide Trp-Trp-Tyr was again employed as a model substrate to allow comparison with the structures determined by NMR (vide supra). Isotopologues Trp(d_5)-Trp-Tyr and Trp-Trp(d_5)-Tyr were synthesized using solution-phase chemistry to incorporate Fmoc-Trp(d_5)-OH in high isotopic purity.[35] Subsequent acylation with template **2** afforded acyclic mixed carbonates **13** and **14** (Fig. 7B). After purification, MS analysis showed >95% average ^2H incorporation at positions indicated in Fig. 7B.

Acidolysis of **13** and **14** under the standard conditions with $MeSO_3H$ proceeded to product mixtures, which were by HPLC–UV, identical to that observed with unlabeled substrate **4**. To avoid potential complications arising from scrambling of the labeling pattern, reactions were analyzed at partial and full conversion, and also under Lewis acidic conditions. The rate of product formation appeared to outcompete scrambling.[36] As anticipated, alkylation of Trp1(d_5) leading to products **8** and **11** was revealed as [M−1] by HPLC–MS analysis of the reaction of **13**. This characteristic mass signature was also observed for products **7**, **10a**, and **10b** arising from alkylation of Trp2(d_5) in the reaction of **14**. While complete retention of deuterium was observed as expected for product **12**, an unexpected loss of two deuterium was found for Trp2 *N*-alkylated product **9** from the acidolysis of **14**. Whether this loss is mechanism based or due to increased exchange rate in the product is not yet known. N-alkylation of indole may accelerate deuterium/hydrogen exchange by enhancing the basic character of the resulting aromatic system.[37] Although this non-diagnostic outcome limits the accuracy of deuterium labeling in probing macrocycle connectivity, this result remains characteristic of substitution at Trp2.

These data demonstrate the utility of deuterium labeled tryptophan in predicting large ring structures arising from aromatic substitution using templates, such as **2** without the need for purification and characterization. This analytical approach may be particularly useful when investigating peptide sequences harboring multiple aromatic amino acids, where spectral overlap can complicate structural assignment. Future development of electrophilic templates incorporating novel or multiple reactive centers may also benefit from similar mass spectrometry-based pre-screens in the search for unique structures.

2.6. Stereochemical assignment and NMR solution structure of pyrroloindoline 12

Macrocyclic pyrroloindoline **12** bears structural resemblance to a large family of natural products possessing these motifs.[38] To our knowledge **12** is the first example possessing an all carbon quaternary center at the core 5,5 ring juncture (Fig. 8A). A number of both naturally and synthetically derived pyrroloindolines have been studied spectroscopically and computationally in an effort to characterize the stability and conformational equilibria of this ring system.[39] Intrigued by this heterocyclic motif in the context of macrocycle **12**, we further examined its structure and three-dimensional conformation using NMR.

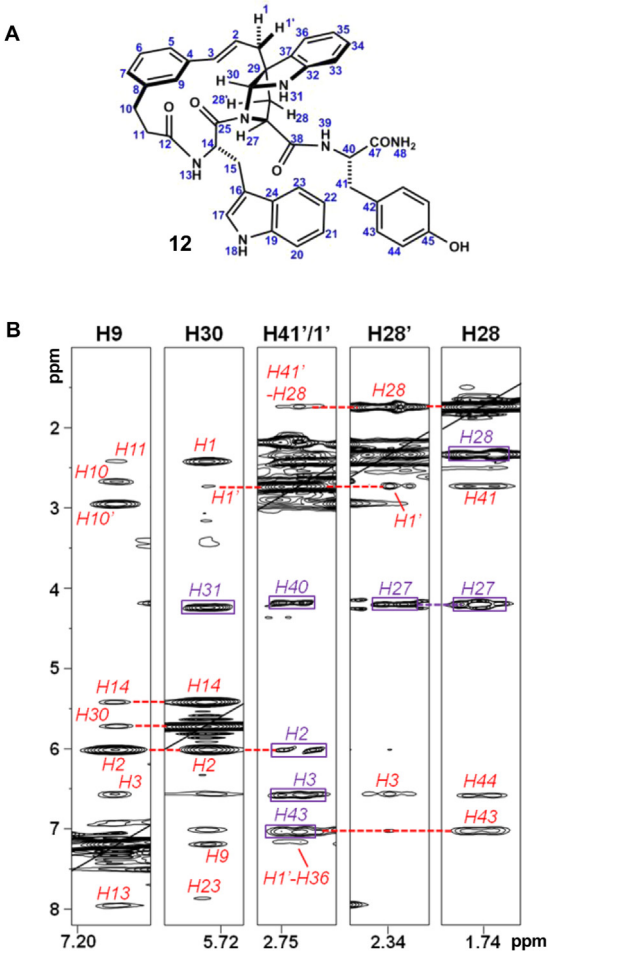

Fig. 8. (A) Numbering scheme used in the annotation of spectra for **12**. (B) Selected slices from 2D-NOESY of compound **12** highlighting intraresidue (purple boxes) and key long-range (red) correlations. Black lines denote the diagonal.

The conformation of **12** in solution appeared to be relatively homogenous. The core pyrroloindoline was clearly observed as a methine, weakly split by the adjacent H31, with a carbon chemical shift of 81.1 ppm characteristic of an aminal. Heteronuclear correlations codified connectivity of the cinnamyl moiety at bridging quaternary center C29. As anticipated, the 5,5 ring juncture was formed with the thermodynamically preferred *cis* relationship, which was readily established from NOE correlation of methine H30 to the geminal pair H1/1′. Spectral overlap in the aliphatic region, and of H27, H31, and H41 frustrated the use of correlations to H1/1′ in assigning the ansa bridge stereochemistry relative to the 27*S* stereocenter, preserved from L-tryptophan. Stereospecific assignment of the geminal pair H28/28′ was tenuous, with no significant difference observed by NOE to H30. Analysis of $^{3}J_{27-28}$ and $^{3}J_{27-28'}$ suggested an *endo* orientation of H28′, which appeared contradictory to their relative chemical shift in comparison to related systems.[39] We viewed a distinct possibility that the macrocyclic motif and/or tyrosine residue could distort this pyrrolidine ring, leading to atypical *J*-values.[40] A single unambiguous long-range NOE from H2 to H27 led to the tentative assignment of the C38-*endo* 27*S*,29*R*,30*R* stereochemistry, as shown. Careful analysis of selective 1D-NOESY, 2D-NOESY, and 2D-ROESY spectra obtained in DMSO or DMSO/D_2O supported this configuration, revealing seven prominent long-range correlations. Notably, strong NOEs within the tetrad H14, H30, H9, and H2 indicated arrangement of these positions along the interior of the macrocycle. An initial model generated from a conformational search incorporating these constraints facilitated assignment of 29 additional long-range NOEs, and calculation of a refined structural ensemble (Fig. 9B) showing agreement with experimental NOEs (see Table S4).

The solution structure revealed several notable features induced by template **2**. Planarity of the cinnamyl unit was retained, as evidenced by strong NOE of H3 to H5, and H2 to H9, thereby limiting the overall conformational flexibility of the 15-membered ring. The Trp1 side chain appeared to populate a single rotamer resulting in a close proximity of the indole ring to the benzene ring of the pyrroloindoline, which was supported by NOE observed between H20 and H33. While side chain torsions were indirectly restrained by long-range NOEs, the calculated rotamer preferences of Trp1 (g^2t^3) and Tyr3 (t^2g^3) agreed only loosely with observed coupling constants ($\pm 30°$), suggesting potential motional averaging at these side chains.[41]

The bridged pyrroloindoline motif formed from cyclization of Trp2 onto the backbone effectively acts as a proline mimic. The backbone amide at this position retains the *trans* configuration, and the highly puckered *endo*-pyrroloindoline induces a turn conformation, analogously to proline, yielding a potential hydrogen bond between the Trp1–C(O) and Tyr3 carboxamide. The anomalous *J*-values associated with H28/28′ were rectified on basis of long-range NOEs from H28 to H43 and H44 indicating a syn relationship of H28 to the C-terminal tyrosine residue, though details of the pyrrolidine ring conformer were not revealed from these force field calculations.[41] These data suggest that compound **12** occupies a relatively ordered conformation in solution that is enforced by both the macrocyclic and pyrroloindoline motifs.

3. Conclusion

In this pilot study, we have demonstrated a template-based approach to form composite macrocyclic peptidomimetics by unique large ring-forming Friedel–Crafts alkylations of tryptophan and tyrosine. A single reaction efficiently accessed eight macrocyclic structures. The product distribution showed a strong dependence on acid promoter and substrate geometry. Rearrangement within a conformationally pre-organized tyrosine O-linked cinnamyl macrocyclic ether favored alkylation *ortho* to the phenol. By reducing the concentration of acid, this product was formed in 20:1 ratio relative to all other isomers. The ability to enhance the formation of specific isomers by tuning the reaction conditions allows rapid access to individual constituents for further study. It should be emphasized that, any one of products **6**–**12** could likely be selectively synthesized de novo utilizing established methodologies.[42]

The peptide domain was found to be conformationally restricted as a result of template-induced macrocycle formation. This was demonstrated in the NMR solution structure of novel *endo*-pyrroloindoline **12** possessing an all carbon quaternary center at ansa bridgehead C29. These results suggest that the

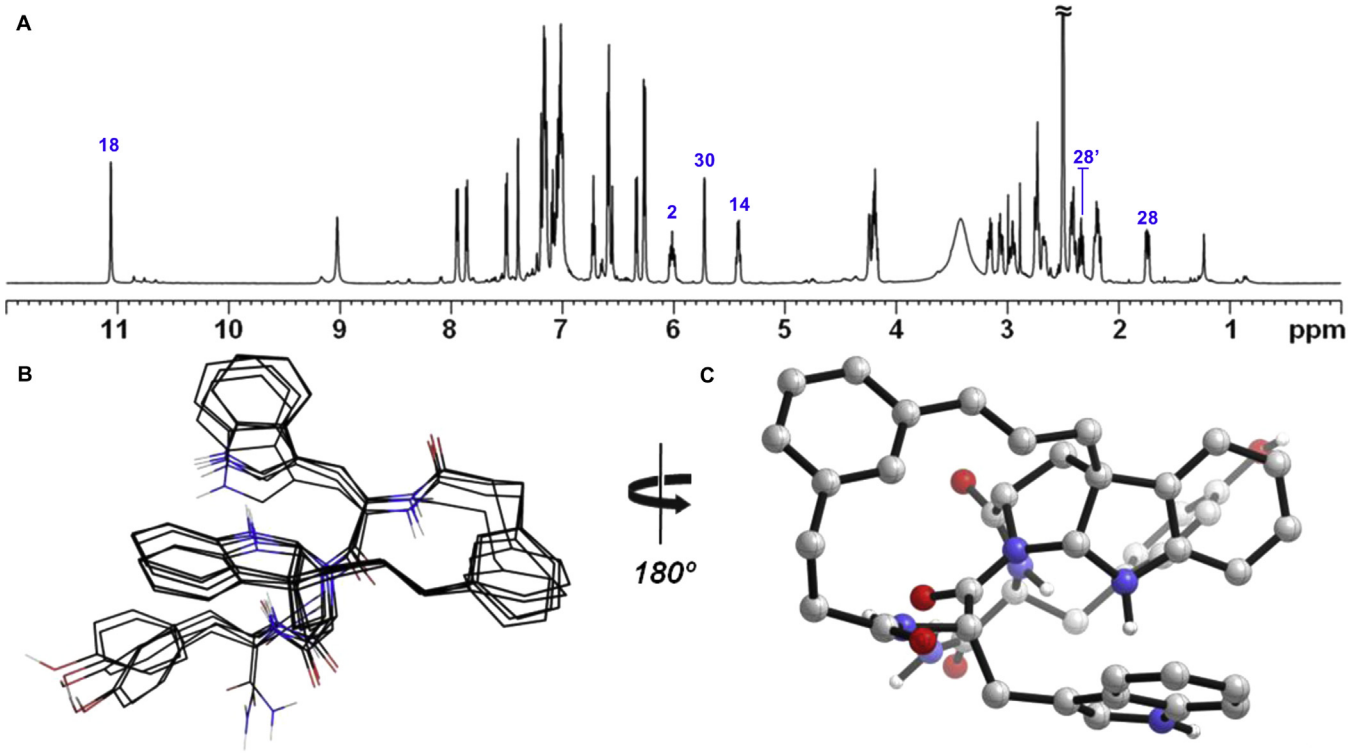

Fig. 9. (A) ^{1}H NMR spectrum of compound **12** (DMSO-d_6, 600 MHz). (B) Overlay of the five lowest energy conformers calculated using NOE distance constrained molecular mechanics simulation and (C) the lowest energy conformer obtained from this analysis. Spectral annotations correspond to numbering scheme in Fig. 8A.

divergent reactivity of templates, such as **2** is an effective means of accessing molecular diversity. Isomeric products inherently possess the same primary peptide sequence, but likely vary substantially in their spatial display of side chains. Products derived from **2**, formed from carbon–carbon sigma bonding, also display improved physicochemical properties. These macrocycles have polar surface area comparable to the linear peptide, but much improved solubility in organic solvents and minimal propensity to aggregate.

We believe divergent strategies, such as those described herein will prove valuable in a broader context of preparing structurally complex peptidomimetics. The particular utility of template **2** is demonstrated by the ability to transform a single peptide, Trp-Trp-Tyr, in two steps into eight isomeric macrocycles that would be otherwise time consuming to prepare. Rapid and efficient syntheses of composite macrocyclic peptidomimetics has the potential to identify small molecules effective against challenging targets where traditional libraries are often unsuccessful. We anticipate methods to generate shape diversity will prove valuable in efforts to recapitulate key motifs within larger folded polypeptides and to target surfaces involved in protein–protein interactions.

4. Experimental

4.1. General remarks

Reactions were performed in air unless otherwise noted. Dichloromethane was dried by passing through an activated alumina solvent drying system. Anhydrous *N*,*N*-dimethylformamide (EMD DriSolv®) was used without further purification. Nitromethane was dried over 4 Å molecular sieves for at least 24 h before use. Methanesulfonic acid (≥99.5%, Sigma Aldrich) was used without further purification. Column chromatography was performed on silica gel 60 (SiliCycle, 240–400 mesh). Thin layer chromatography (TLC) utilized pre-coated plates (Sorbent Technologies, silica gel 60 PF254, 0.25 mm) visualized with UV 245 nm, iodine, or basic potassium permanganate stain.

Purification of acidolysis products employed an Agilent 1100/1200 HPLC system equipped with G1361A preparative pumps, a G1314A autosampler, a G1314A VWD, and a G1364B automated fraction collector. Analytical HPLC was performed using the same system, but with a G1312A binary pump. Mass spectra were recorded using an Agilent 6130 LC/MS system equipped with an ESI source. High-resolution mass spectra were recorded at the UCLA Molecular Instrumentation Center on a Waters LCT Premier equipped with an Acquity LC and Autosampler.

4.2. NMR methods

NMR spectra were recorded on Bruker Avance (500 or 600 MHz) spectrometers. Data for ^{1}H NMR spectra are reported as follows: chemical shift (δ parts per million) (multiplicity, coupling constant (Hertz), integration), and are referenced to a residual protonated solvent peak.[43] ^{13}C resonances are reported in terms of chemical shift (δ ppm) as referenced to DMSO-d_6. For mass-limited samples, solvent magnetic susceptibility matched Shigemi tubes were used with a sample volume of ~300 μL. Optimization of on-axis shims was accomplished using the TopShim automated tool within Bruker Topspin™ 2.1. Optimization of off-axis shims was performed manually.[44] ^{1}H 90° transmitter pulse lengths were calibrated by back calculation from the 360° or 180° null.[45] The pulse width or power level for soft pulses and shaped pulses were calculated using the Shape Tool within TopSpin™ 2.1. ^{1}H–^{1}H COSY spectra were recorded using a phase sensitive, gradient enhanced double-quantum-filtered experiment, using States-TPPI acquisition.[46] TOCSY spectra were recorded using a sensitivity improved, phase sensitive experiment using a 60 ms DIPSI-2 pulse train for homonuclear Hartman–Hahn transfer.[47] NOESY spectra were recorded using a phase sensitive experiment with selection gradients during the mixing time.[48] ROESY spectra were recorded using a phase sensitive

experiment with selection gradients and water suppression with excitation sculpting.[49] Carbon chemical shifts were measured from 2D plots of either HSQC spectra for protonated carbons or HMBC spectra for non-protonated carbons. $^{1}H-^{13}C$ HSQC spectra were recorded using a sensitivity improved phase sensitive experiment using an adiabatic shape pulse for ^{13}C inversion, and ^{13}C decoupling during acquisition.[50] Experimental parameters were optimized for $^{1}J_{CH}$=145 Hz. $^{1}H-^{13}C$ HMBC spectra were recorded using a gradient selected experiment with a two-fold J-filter optimized for $^{1}J_{CH}$=125–165 Hz. Experimental parameters were optimized for long-range $^{n}J_{CH}$=8 Hz.

4.3. Synthesis of compounds 4–12

*4.3.1. Acylation of Trp-Trp-Tyr with template **2**—preparation of **4**.* An oven-dried, screw-capped scintillation vial was charged with Trp-Trp-Tyr·TFA (343 mg, 0.515 mmol) and *N*-hydroxysuccinimidyl ester **2** (208 mg, 0.515 mmol) followed by addition of anhydrous DMF (10 ml) and $^{i}Pr_2NEt$ (359 μl, 2.06 mmol). The reaction was allowed to stir at room temperature for 3 h. The DMF was removed by rotary evaporation and the residue was dissolved in MeCN/$CHCl_3$ (1:3) and purified by column chromatography (SiO_2, gradient 0–10% MeOH/$CHCl_3$) to give **4** as a white solid (337 mg, 0.402 mmol, 78%). ^{1}H NMR (DMSO-d_6, 600 MHz): δ 10.79 (d, J=1.8 Hz, 1H), 10.7 (d, J=1.6 Hz, 1H), 9.13 (br s, 1H), 8.07 (d, J=7.6 Hz, 1H), 8.00 (d, J=8.0 Hz, 1H), 7.81 (d, J=8.1 Hz, 1H), 7.56 (d, J=7.8 Hz, 1H), 7.49 (d, J=7.8 Hz, 1H), 7.3 (d, J=5.2 Hz, 1H), 7.28 (d, J=5.3 Hz, 1H), 7.21–7.26 (m, 2H), 7.18 (br s, 1H), 7.15 (dd, J=7.7, 7.7 Hz, 1H), 7.00–7.08 (m, 5H), 6.91–6.99 (m, 5H), 6.62 (d, J=8.6 Hz, 2H), 6.57 (d, J=16.1 Hz, 1H), 6.29 (dt, J=16.0, 6.2 Hz, 1H), 4.63 (dd, J=6.2, 1.0 Hz, 2H), 4.43–4.54 (m, 2H), 4.35 (ddd, J=7.9, 7.9, 5.8 Hz, 1H), 3.06 (d, J=4.6 Hz, 1H), 3.03 (d, J=4.3 Hz, 1H), 2.93 (dd, J=14.8, 8.6 Hz, 1H), 2.79–2.88 (m, 2H), 2.71 (dd, J=13.9, 7.8 Hz, 1H), 2.57–2.62 (m, 2H), 2.23–2.30 (m, 2H), 1.14 (s, 9H). ^{13}C NMR (DMSO-d_6, 150 MHz): δ 173.2, 172.3, 171.9, 171.4, 156.3, 153.3, 142.2, 136.5, 136.5, 136.3, 133.9, 130.6, 129.1, 128.4, 128.2, 127.83, 127.80, 126.9, 124.6, 124.0, 123.7, 121.29, 121.27, 119.0, 118.8, 118.7, 118.6, 115.3, 111.72, 111.68, 110.7, 110.4, 82.0, 67.4, 54.5, 54.2, 53.8, 37.33, 37.28, 31.4, 28.0, 27.85, 27.78. HRMS (ESI) calculated for $C_{48}H_{52}N_6O_8$ $[M+Na]^+$: 863.3745, found 863.3757.

*4.3.2. Pd-catalyzed macrocyclization—preparation of **5**.* A solution of acyclic carbonate 4 (109 mg, 0.130 mmol) in DMF (26 ml, 5 mM) was sparged with argon for 15 min. The septum was removed briefly to allow the addition of $Pd(PPh_3)_4$ (8 mg, 0.0065 mmol, 5 mol %). The mixture was stirred for 1 h at which point analysis by HPLC–UV showed complete conversion of 4–5. Silica bound thiol (Si-Thiol, Silicycle, 1.29 mmol/g, ~25 mg) was added to the reaction mixture, mixed for 5 min, and filtered. DMF was removed by rotary evaporation in vacuo. The residual oil was taken up in $CHCl_3$/MeCN and purified by column chromatography (SiO_2, gradient 0–10% MeOH/$CHCl_3$) to give **5** as a white solid (67 mg, 0.092 mmol, 71%). ^{1}H NMR (DMSO-d_6, 500 MHz): δ 10.7 (d, J=2.0 Hz, 1H), 10.64 (d, J=2.0 Hz, 1H), 7.99 (d, J=8.1 Hz, 1H), 7.83 (d, J=7.9 Hz, 1H), 7.51 (d, J=8.0 Hz, 1H), 7.48 (d, J=7.8 Hz, 1H), 7.46 (d, J=8.0 Hz, 1H), 7.28 (br d, J=3.7 Hz, 1H), 7.26 (br d, J=3.9 Hz, 1H), 7.24 (br s, 1H), 7.10–7.13 (m, 3H), 6.99–7.10 (m, 6H), 6.90–6.96 (m, 3H), 6.74 (d, J=8.9 Hz, 2H), 6.6 (d, J=2.5 Hz, 1H), 6.47 (br d, J=16.1 Hz, 1H), 6.21 (dt, J=15.9, 5.9 Hz, 1H), 4.68 (dd, J=15.3, 6.3 Hz, 1H), 4.6 (dd, J=14.3, 5.6 Hz, 1H), 4.51 (ddd, J=7.6, 7.6, 5.9 Hz, 1H), 4.34 (ddd, J=10.9, 8.1, 2.8 Hz, 1H), 4.22 (app q, J=7.5 Hz, 1H), 3.02 (dd, J=14.8, 5.5 Hz, 1H), 2.92 (dd, J=13.8, 2.6 Hz, 1H), 2.84 (dd, J=14.7, 6.0 Hz, 1H), 2.70–2.77 (m, 4H), 2.59 (dd, J=14.8, 7.8 Hz, 1H), 2.42–2.47 (m, 1H), 2.24–2.32 (m, 1H). ^{13}C NMR (DMSO-d_6, 125 MHz): δ 173.9, 171.9, 171.4, 171.2, 157.0, 141.6, 136.4, 136.3, 133.4, 130.6, 130.3, 128.8, 127.9, 127.8, 126.1, 125.4, 124.8, 124.1, 124.0, 121.3, 121.2, 118.9, 118.8, 118.6, 115.1, 111.70, 111.66, 110.5, 110.3, 68.2, 54.8, 54.1, 53.5, 36.8, 35.9, 30.6, 28.0, 27.5. HRMS (ESI) calculated for $C_{43}H_{42}N_6O_5$ $[M+H]^+$: 723.3295, found 723.3276.

*4.3.3. Acidolysis of macrocycle **5**—preparation of **6**–**12**.* Tyrosine macroether **5** (80 mg, 0.11 mmol) was suspended in dry nitromethane (22 ml, 5 mM) under an argon atmosphere, and treated with methanesulfonic acid (108 μl, 1.66 mmol, 15 equiv) at room temperature, which caused complete dissolution of the starting material. After 2 h the reaction was partitioned between EtOAc and saturated $NaHCO_3$. The organic phase was washed with saturated $NaHCO_3$ (×2) and brine, then dried over Na_2SO_4, and concentrated. The product mixture was reconstituted in DMF and purified by semi-preparative RP-HPLC (Sunfire C18, 5 μm, 10×250 mm, gradient: 41 →48% MeCN/H_2O, 0.1% TFA, 21 min). Fractions were pooled and concentrated under reduced pressure using a Thermo Savant SC250EXP Speedvac.

*4.3.4. Acidolysis of acyclic carbonate **4**—preparation of **6**–**12**.* Acyclic cinnamyl carbonate (**4**) (330 mg, 0.39 mmol) was suspended in dry nitromethane (78 ml, 5 mM) under an argon atmosphere, and treated with methanesulfonic acid (382 μl, 5.89 mmol, 15 equiv) at room temperature, which caused complete dissolution of the starting material. After 2 h the reaction was worked up and purified as in Section 4.3.3. HRMS (ESI) calculated for $C_{43}H_{42}N_6O_5$ $[M+H]^+$: 723.3295, found 723.3278 (**7**). HRMS (ESI) calculated for $C_{43}H_{42}N_6O_5$ $[M+Na]^+$: 745.3115, found 745.3118 (**6**), 745.3117 (**8**), 745.3115 (**9**), 745.3121 (**10a**/**b**), 745.3127 (**11**), 745.3127 (**12**).

Acknowledgements

Funding was provided by the National Cancer Institute (PO1 CA95471) and the Donald J. & Jane M. Cram Endowment, the NSF Graduate Research Fellowship DGE-0707424 (fellowship to T.E.R.) and a major instrumentation grant from the National Science Foundation (CHE-1048804). We gratefully acknowledge Dr. Robert Peterson and Dr. Robert Taylor for expert assistance in obtaining NMR correlation spectra.

Supplementary data

Supplementary data related to this article can be found at http://dx.doi.org/10.1016/j.tet.2013.05.060.

References and notes

1. (a) Mallinson, J.; Collins, I. *Future Med. Chem.* **2012**, *4*, 1409–1438; (b) Schreiber, S. L. *Science* **2000**, *287*, 1964–1969; (c) Payne, D. J.; Gwynn, M. N.; Holmes, D. J.; Pompliano, D. L. *Nat. Rev. Drug Discovery* **2007**, *6*, 29–40; (d) Chanda, S. K.; Caldwell, J. S. *Drug Discovery Today* **2003**, *8*, 168–174.
2. (a) Wells, J. A.; McClendon, C. L. *Nature* **2007**, *450*, 1001–1009; (b) Spencer, R. W. *Biotechnol. Bioeng.* **1998**, *61*, 61–67; (c) Verdine, G. L.; Walensky, L. D. *Clin. Cancer Res.* **2007**, *13*, 7264–7270; (d) Arkin, M. R.; Wells, J. A. *Nat. Rev. Drug. Discovery* **2004**, *3*, 301–317; (e) Guo, C.; Hou, X.; Dong, L.; Dagostino, E.; Greasley, S.; Ferre, R.; Marakovits, J.; Johnson, M. C.; Matthews, D.; Mrockowski, B.; Parge, H.; VanArsdale, T.; Popoff, I.; Piraino, J.; Margosiak, S.; Thomson, J.; Los, G.; Murray, B. W. *Bioorg. Med. Chem. Lett.* **2009**, *19*, 5613–5616.
3. (a) Sundberg, E. J.; Mariuzza, R. A. *Structure* **2000**, *8*, R137–R142; (b) Lo Conte, L.; Chothia, C.; Janin, J. *J. Mol. Biol.* **1999**, *5*, 2177–2198; (c) Sarmiento, M.; Puius, Y. A.; Vetter, S. W.; Keng, Y. F.; Wu, L.; Zhao, Y.; Lawrence, D. S.; Almo, S. C.; Zhang, Z. Y. *Biochemistry* **2000**, *39*, 8171–8179; (d) Eyrisch, S.; Helms, V. *J. Med. Chem.* **2007**, *50*, 3457–3464.
4. (a) Thanos, C. D.; De Lano, W. L.; Wells, J. A. *Proc. Natl. Acad. Sci. U.S.A.* **2006**, *103*, 15422–15427; (b) Friberg, A.; Vigil, D.; Zhao, B.; Daniels, R. N.; Burke, J. P.; Garcia-Barrantes, P. M.; Camper, D.; Chauder, B. A.; Lee, T.; Olejniczak, E. T.; Fesik, S. W. *J. Med. Chem.* **2013**, *56*, 15–30; (c) Zhao, H.; Liu, L.; Huan, J.; Bernard, D.; Karatas, H.; Navarro, A.; Lei, M.; Wang, S. *J. Med. Chem.* **2013**, *56*, 1113–1123.
5. (a) Pillutla, R. C.; Hsiao, K.-C.; Beasley, J. R.; Brandt, J.; Østergaard, S.; Hansen, P. H.; Spetzler, J. C.; Danielsen, G. M.; Andersen, A. S.; Brissette, R. E.; Lennick, M.; Fletcher, P. W.; Blume, A. J.; Schäffer, L.; Goldstein, N. I. *J. Biol. Chem.* **2002**, *277*, 22590–22594; (b) Bogan, A. A.; Thorn, K. S. *J. Mol. Biol.* **1998**, *280*, 1–9; (c) Moreira, I. S.; Fernandes, P. A.; Ramos, M. J. *Proteins* **2007**, *68*, 803–812.

6. (a) Sidhu, S. S.; Fairbrother, W. J.; Deshayes, K. *ChemBioChem* **2003**, *4*, 14–25; (b) Wrighton, N. C.; Farrell, F. X.; Chang, R.; Kashyap, A. K.; Barbone, F. P.; Mulcahy, L. S.; Johnson, D. L.; Barrett, R. W.; Jolliffe, L. K.; Dower, W. J. *Science* **1996**, *273*, 458–464; (c) Fairbrother, W.; Christinger, H. W.; Cochram, A. G.; Fuh, G.; Keenan, C. J.; Quan, C.; Shriver, S.; Tom, J. Y. K.; Wells, J. A.; Cunningham, B. C. *Biochemistry* **1998**, *37*, 17754–17764.
7. (a) Sato, A. K.; Viswanathan, M.; Kent, R. B.; Wood, C. R. *Curr. Opin. Biotechnol.* **2006**, *17*, 638–642; (b) White, T. R.; Renzelman, C. M.; Rand, A. C.; Rezai, T.; McEwen, C. M.; Gelev, V. M.; Linington, R. G.; Leung, S. S. F.; Kalgutkar, A. S.; Bauman, J. N.; Zhang, Y.; Liras, S.; Price, D.; Mathiowetz, A. M.; Jacobson, M. P.; Lokey, R. S. *Nat. Chem. Biol.* **2011**, *7*, 810–817; (c) Bursavich, M. G.; Rich, D. H. *J. Med. Chem.* **2002**, *45*, 541–558.
8. Schumacher, T. N. M.; Mayr, L. M.; Minor, D. L., Jr.; Milhollen, M. A.; Burgess, M. W.; Kim, P. S. *Science* **1996**, *271*, 1854–1857.
9. Olsen, C. A.; Montero, A.; Leman, L. J.; Ghadiri, M. R. *ACS Med. Chem. Lett.* **2012**, *3*, 749–753.
10. (a) Thakkar, A.; Trinh, T. B.; Pei, D. *ACS Comb. Sci.* **2013**, *15*, 120–129; (b) Fluxa, V. S.; Reymond, J.-L. *Bioorg. Med. Chem.* **2009**, *17*, 1018–1025.
11. White, C. J.; Yudin, A. K. *Nat. Chem.* **2011**, *3*, 509–524.
12. Zhao, H.; Negash, L.; Wei, Q.; LaCour, T. G.; Estil, S. J.; Capota, E.; Pieper, A. A.; Harran, P. G. *J. Am. Chem. Soc.* **2008**, *130*, 13864–13866.
13. Lawson, K. V.; Rose, T. E.; Harran, P. G. *Tetrahedron Lett.* **2011**, *52*, 653–654.
14. Widely adopted methods include lactamization (a), azide–alkyne cycloaddition (b), 'native chemical ligation' (c), and ring-closing olefin metathesis (d): (a) Pehere, A. D.; Abell, A. D. *Org. Lett.* **2012**, *14*, 1330–1333; (b) Zhang, L.; Tam, J. P. *J. Am. Chem. Soc.* **1997**, *119* 2636–2370; (c) Blackwell, H. E.; Grubbs, R. H. *Angew. Chem., Int. Ed.* **1998**, *37*, 3281–3284.
15. Several noteworthy macrocyclization strategies have recently been reported: (a) Dong, H.; Limberakis, C.; Liras, S.; Price, D.; James, K. *Chem. Commun.* **2012**, 11644–11646; (b) Collins, J. C.; Farley, K. A.; Limberakis, C.; Liras, S.; Price, D.; James, K. *J. Org. Chem.* **2012**, *77*, 11079–11090; (c) Londregan, A. T.; Farley, K. A.; Limberakis, C.; Mullins, P. B.; Piotrowski, D. W. *Org. Lett.* **2012**, *14*, 2890–2893; (d) Meyer, F.-M.; Collins, J. C.; Borin, B.; Liras, S.; Limberakis, C.; Mathiowetz, A. M.; Philippe, L.; Price, D.; Song, K.; James, K. *J. Org. Chem.* **2012**, *77*, 3099–3114; (e) Hili, R.; Rai, V.; Yudin, A. K. *J. Am. Chem. Soc.* **2010**, *132*, 2889–2891.
16. Wei, Q.; Harran, S.; Harran, P. G. *Tetrahedron* **2003**, *45*, 8947–8954.
17. The detailed preparation of **2** will be reported elsewhere: Lawson, K. V.; Rose, T. E.; Harran, P. G., submitted for publication.
18. The use of divergent reactions to access molecular diversity is also manifest in the synthesis of combinatorial one bead, one compound libraries (a), split-pool synthesis (b), or mixture-based libraries (c), (d), (e), here varying only in the way mixtures are generated and manipulated, and the methods by which desirable individual constituents are obtained: (a) Lam, K. S.; Salmon, S. E.; Hersh, E. M.; Hruby, V. J.; Kazmierski, W. M.; Knapp, R. J. *Nature* **1991**, *354*, 82–84; (b) Furka, A.; Sebastyén, F.; Dibó, G. *Int. J. Pept. Protein Res.* **1991**, *37*, 487–493; (c) Houghten, R. A.; Pinilla, C.; Blondelle, S. E.; Appel, J. R.; Dooley, C. T.; Cuervo, J. H. *Nature* **1991**, *354*, 84–86; (d) Boger, D. L.; Fink, B. E.; Hedrick, M. P. *J. Am. Chem. Soc.* **2000**, *122*, 6382–6394; (e) Pinilla, C.; Appel, J. R.; Borràs, E.; Houghten, R. A. *Nat. Med.* **2003**, *9*, 118–122.
19. Constraining side-chain conformations in synthetic peptidomimetics has been found advantageous: (a) Hruby, V. J.; Li, G.; Haskell-Luevano, C.; Shenderovich, M. *Biopolymers* **1997**, *43*, 219–266; (b) Hruby, V. J. *Life Sci.* **1993**, *31*, 189–199; (c) Hruby, V. J.; Al-Obeidi, F.; Kazmierski, W. *Biochem. J.* **1990**, *268*, 249–262.
20. (a) Bermel, W.; Griesinger, C.; Kessler, H.; Wagner, K. *Magn. Reson. Chem.* **1987**, *25*, 325–326; (b) Kessler, H.; Griesinger, C.; Zarbock, J.; Lossli, H. R. *J. Magn. Reson.* **1984**, *57*, 331–336.
21. (a) Chazin, W. J.; Wright, P. E. *Biopolymers* **1987**, *26*, 973–977; (b) Wütrich, K. *Biopolymers* **1983**, *22*, 131–138.
22. Bax, A.; Davis, D. G. *J. Magn. Reson.* **1985**, *65*, 355–360.
23. Large ring-forming Friedel–Crafts alkylations have been used on occasion to prepare paracyclophanes and pillararenes: (a) Gribble, G. W.; Nutaitis, C. F. *Tetrahedron Lett.* **1985**, *26*, 6023–6026; (b) Holler, M.; Allenbach, N.; Sonet, J.; Nuerengarten, F. *Chem. Commun.* **2012**, 2576–2578; (c) Ogoshi, T.; Kanai, S.; Fujinami, S.; Yamagashi, T.; Nakamoto, Y. *J. Am. Chem. Soc.* **2008**, *130*, 5022–5023.
24. Friedel–Crafts type large-ring forming acylations are known: (a) Huisgen, R.; Rapp, W.; Ugi, I.; Walz, H.; Glogger, I. *Justus Liebigs Ann. Chem.* **1954**, *586*, 52–69; (b) Taitis, S. Z.; Belen'kii, L. I.; Gol'dfarb, Y. L. *B. Acad. Sci. USSR CH+* **1963**, *12*, 1328–1334; (c) Galli, C.; Illuminati, G.; Mandolini, L. *J. Org. Chem.* **1980**, *45*, 311–315; (d) Chen, M.; Guzei, I.; Rheingold, A. L.; Gibson, H. W. *Macromolecules* **1997**, *30*, 2516–2518; (e) Yuan, Y.; Men, H.; Lee, C. *J. Am. Chem. Soc.* **2004**, *126*, 14720–14721.
25. (a) Demopoulos, V. J.; Nicolaou, I. *Synthesis* **1998**, 1519–1522; (b) Li, J.; Li, B.; Chen, X.; Zhang, G. *Synlett* **2003**, 1447–1450; (c) Murakami, Y.; Tani, M.; Tanaka, K.; Yokoyama, Y. *Heterocycles* **1984**, *22*, 241–244; (d) Schmit Pérez, M. C.; Jubert, A. H.; Vitale, A.; Lobayan, R. M. *J. Mol. Model.* **2011**, *17*, 1227–1239.
26. Taniguchi, M.; Hino, T. *Tetrahedron* **1981**, *8*, 1487–1494.
27. (a) Brown, H. C.; Jungk, H. *J. Am. Chem. Soc.* **1955**, *77*, 5584–5589; (b) Weiss, R.; Kölbl, H.; Schlierf, C. *J. Org. Chem.* **1976**, *41*, 2258–2261; (c) Olah, G. A.; Flood, S. H.; Kuhn, S. J.; Moffatt, M. E.; Overchuck, N. A. *J. Am. Chem. Soc.* **1964**, *86*, 1046–1054; (d) Olah, G. A. *Acc. Chem. Res.* **1971**, *4*, 240–248.
28. (a) Olah, G. A.; Kuhn, S. J.; Flood, S. H. *J. Am. Chem. Soc.* **1962**, *84*, 1688–1695; (b) Gore, P. G. In *Friedel–Crafts and Related Reactions*; Olah, G. A., Ed.; Interscience: New York, NY, 1964; Vol. III; (c) Keumi, T.; Nakamura, M.; Kitamura, M.; Tomioka, N.; Kitajima, H. *J. Chem. Soc., Perkin Trans. 2* **1985**, 909–913; (d) Keumi, T.; Yagi, Y.; Kato, Y.; Taniguchi, R.; Tempōrin, M.; Kitajima, H. *J. Chem. Soc., Perkin Trans. 2* **1984**, 799–805.
29. A possible, though less likely in our opinion, path from **5** to **6** under these conditions would involve the transient formation of a branched aryl allylic ether that subsequently undergoes acid-promoted sigmatropic rearrangement. Svanholm, U.; Parker, V. D. *J. Chem. Soc., Perkin Trans. 2* **1974**, 169–173.
30. Rice, F. O.; Teller, E. *J. Chem. Phys.* **1938**, *6*, 489–496.
31. Hine, J. *J. Org. Chem.* **1966**, *31*, 1236–1244.
32. Data is consistent with an intermediate phenylallyl carbocation: (a) Goering, H. L.; Dilgren, R. E. *J. Am. Chem. Soc.* **1960**, *82*, 5744–5749; (b) Goering, H. L.; Linsay, E. C. *J. Am. Chem. Soc.* **1969**, *91*, 7435–7439; (c) Ref. 28a.
33. (a) Winstein, S.; Clippinger, E.; Fainberg, A. H.; Heck, R.; Robinson, G. C. *J. Am. Chem. Soc.* **1956**, *78*, 328–335; (b) Valkanas, G.; Waight, E. S.; Weinstock, M. *J. Chem. Soc.* **1963**, 4248–4256.
34. (a) Denney, D. B.; Klemchuk, P. P. *J. Am. Chem. Soc.* **1958**, *80*, 6014–6016; (b) Fürstner, A.; Voigtländer, D.; Schrader, W.; Giebel, D.; Reetz, M. T. *Org. Lett.* **2001**, *3*, 417–420.
35. Sheppeck, J. E., II; Kar, H.; Hong, H. *Tetrahedron Lett.* **2000**, *41*, 5329–5333.
36. H-Trp(d_5)-OH subjected to $MeSO_3H$ (15 equiv) in $MeNO_2$ showed considerable $^2H/H$ exchange at 16 h. Early time points (10 min) did not show exchange, indicating the rate of macrocyclization would outcompete deuterium scrambling. When H-Trp(d_5)-OH was exposed to $Sc(OTf)_3$ in $MeNO_2$, no $^2H/H$ exchange was observed even at extended reaction times (16 h). The anomalous loss of two mass units [M−2] from acidolysis of **13** to form labeled **9** could not be observed with $Sc(OTf)_3$ as **9** is formed in only trace quantities under these conditions.
37. (a) Hinman, R. L.; Whipple, E. D. *J. Am. Chem. Soc.* **1962**, *84*, 2534–2539; (b) Hinman, R. L.; Lang, J. *J. Am. Chem. Soc.* **1964**, *86*, 3796–3806.
38. Ruiz-Sanchis, P.; Savina, S. A.; Albericio, F.; Álvarez, M. *Chem.—Eur. J.* **2011**, *17*, 1388–1408.
39. (a) Marles-Ríos, M. S.; Santos-Sánchez; Suárez-Castillo, O. R.; Joseph-Nathan, P. *Magn. Reson. Chem.* **2002**, *40*, 677–682; (b) Crich, D.; Chan, C. O.; Davies, J. W.; Natarajan, S.; Vinter, J. G. *J. Chem. Soc., Perkin Trans. 2* **1992**, 2233–2240.
40. For detailed discussion of dynamics and NMR characterization of 5five-membered rings, see: (a) Napolitano, J. G.; Gavín, J. A.; García, C.; Norte, M.; Fernández, J. J.; Hernández Daranas, A. *Chem.—Eur. J.* **2011**, *17*, 6338–6347; (b) Altona, C.; Sundaralingam, M. *J. Am. Chem. Soc.* **1972**, *95*, 2333–2344.
41. Hybers, S. G.; Märki, W.; Wagner, G. *Eur. J. Biochem.* **1987**, *164* 625–635.
42. For catalyzed cross-couplings to form allylated arenes see: (a) Fürstner, A.; Seidel, G. *Synlett* **1998**, 161–162; (b) Anka-Lufford, L. L.; Prinsell, M. R.; Weix, D. J. *J. Org. Chem.* **2012**, *77*, 9989–10000 For synthesis of C-3 allylated pyrroloindolines see: (c) Kimura, M.; Futamata, M.; Mukai, R.; Tamaru, Y. *J. Am. Chem. Soc.* **2005**, *127*, 4592–4593.
43. Gottlieb, H. E.; Kotlyar, V.; Nudelman, A. *J. Org. Chem.* **1997**, *62*, 7512–7515.
44. Berger, S.; Braun, S. *200 and More NMR Experiments*; Wiley-VCH: Weinheim, Germany, 2004; pp. 6–11.
45. (a) Claridge, T. D. W. *High-Resolution NMR Techniques in Organic Chemistry*; Pergamon: Oxford, UK, 1999; pp. 94–97; (b) Berger, S.; Braun, S. *200 and More NMR Experiments*; Wiley-VCH: Weinheim, Germany, 2004; pp. 15–17.
46. (a) Hurd, R. E. *J. Magn. Reson.* **1990**, *87*, 422–428; (b) Brereton, I. M.; Crozier, S.; Field, J.; Doddrell, D. M. *J. Magn. Reson.* **1991**, *93*, 54–62; (c) Shaw, A. A.; Salaun, C.; Dauphin, J. F.; Ancian, B. *J. Magn. Reson., Ser. A* **1996**, *120*, 110–115.
47. Cavanagh, J.; Rance, M. *J. Magn. Reson.* **1990**, *88*, 72–85.
48. Wagner, R.; Berger, S. *J. Magn. Reson., Ser. A* **1996**, *123*, 119–121.
49. (a) Bax, A.; Davis, D. G. *J. Magn. Reson.* **1985**, *63*, 207–213; (b) Hwang, T. L.; Shaka, A. J. *J. Magn. Reson., Ser. A* **1995**, *112*, 275–279.
50. (a) Palmer, A. G., III; Cavanagh, J.; Wright, P. E.; Rance, M. *J. Magn. Reson.* **1991**, *93*, 151–170; (b) Kay, L. E.; Keifer, P.; Saarinen, T. *J. Am. Chem. Soc.* **1992**, *114*, 10663–10665; (c) Schleucher, J.; Schwendinger, M.; Sattler, M.; Schmidt, P.; Schedletzky, O.; Glaser, S. J.; Sorensen, O. W.; Griesinger, C. *J. Biomol. NMR* **1994**, *4*, 301–306.